Ann Nucl Med (2008) 22:417–424
DOI 10.1007/s12149-008-0136-1

ORIGINAL ARTICLE

In vivo imaging of microglial activation using a peripheral benzodiazepine receptor ligand: [^{11}C]PK-11195 and animal PET following ethanol injury in rat striatum

**Hiroshi Toyama · Kentaro Hatano · Hiromi Suzuki
Masanori Ichise · Sotaro Momosaki · Gen Kudo
Fumitaka Ito · Takashi Kato · Hiroshi Yamaguchi
Kazuhiro Katada · Makoto Sawada · Kengo Ito**

Received: 12 December 2007 / Accepted: 19 February 2008

Abstract
Objective To investigate whether [^{11}C]PK-11195, a specific peripheral benzodiazepine receptors (PBRs) ligand for positron emission tomography (PET), can show activated microglia in a rat brain injury model.
Methods On day 1, ethanol was injected into the rat's right striatum (ST) using a stereotaxic operative procedure. On day 3, head magnetic resonance imaging (MRI) scans for surgically treated rats were performed to evaluate ethanol injury morphologically. On day 4, dynamic PET scans (17 injured rats and 7 non-injured controls) were performed for 60 min with an animal PET scanner under chloral hydrate anesthesia following a bolus injection of [^{11}C]PK-11195 through tail vein. Because PBRs are present throughout the brain, there is no suitable receptor-free reference region. The reference tissue model may not be applicable because of low target to background ratio for low affinity of [^{11}C]PK-11195 to PBRs. We evaluated the PBRs binding with regions of interest (ROIs)-based approach to estimate total distribution volume (V). We used an integral from 0 min to 60 min (V_{60}) as an estimate of V. On the coronal PET image, ROIs were placed on bilateral ST. Differences in right/left ST V_{60} ratios between lesioned and unlesioned control rats were compared using unpaired t tests. Immunohistochemical staining was performed for confirming the presence of activated microglia following decapitation on the PET experiment day.
Results The right/left ST V_{60} ratios in lesioned rats (1.07 ± 0.08) were significantly higher than those in unlesioned control rats (1.00 ± 0.06, $P < 0.05$). On immunohistochemical staining, activated microglia were exclusively observed in the injured right ST but not in the non-injured left ST of the injury rats and the bilateral ST of the non-injured control rats.
Conclusions These results suggest that [^{11}C]PK-11195 PET imaging would be a useful tool for evaluating microglial activation in a rat brain injury model.

Keywords Animal PET · Microglia · [^{11}C]PK-11195 · Peripheral benzodiazepine receptors · Rat

H. Toyama (✉) · G. Kudo · F. Ito · K. Katada
Department of Radiology, Fujita Health University, 1-98 Dengakugakubo, Kutsukake, Toyoake, Aichi 470-1192, Japan
e-mail: htoyama@fujita-hu.ac.jp

K. Hatano · S. Momosaki · T. Kato · H. Yamaguchi · K. Ito
Department of Brain Science and Molecular Imaging, National Institute for Longevity Sciences, Obu, Japan

H. Suzuki · M. Sawada
Department of Brain Life Science, Research Institute of Environmental Medicine, Nagoya University, Nagoya, Japan

M. Ichise
Department of Radiology, Columbia University, New York, NY, USA

Introduction

In the central nervous system (CNS), microglia are major glial components and become activated in response to a wide variety of pathological stimuli such as brain injury and degeneration [1–3]. There is increasing evidence that microglia play an active part in degenerative CNS diseases. In Alzheimer's disease (AD), activated microglia appear to be involved with the plaque formation [2]. In the normal adult CNS, microglia constitute relatively stable cell population [4]. The activated microglial cell

following injury or degeneration undergoes morphological transformation [4]. The transition of microglia from the normal resting state to the activated state is also associated with an increased expression of receptors known as peripheral benzodiazepine receptors (PBRs). Because PBRs are very few in resting microglia, increased PBRs may be used as a marker for detecting activated microglia in vivo, which in turn may be a marker for an active inflammatory disease in the brain [1]. Positron emission tomography (PET) imaging of microglial activation using [^{11}C]PK-11195, a specific PBRs ligand, has been investigated in several neurological conditions such as Parkinson's disease animal model [5], AD [6], and HIV-associated dementia [7] in humans. [^{11}C]PK-11195 with a relatively low affinity for the PBRs is unfortunately unable to show any significant signals from low PBRs densities in the normal brain with inactivated microglia [8–10]. However, the absence of signals in the normal brain does not imply that there are no PBRs in the brain. In contrast, PBRs are widely distributed throughout the normal brain [4]. Here, there is actually no brain tissue devoid of receptors (reference tissue). In this situation with no reference tissue, traditionally a total distribution volume (V) has been used as a PET-measured receptor parameter. However, the estimation of V usually requires invasive arterial blood sampling and tracer metabolite analysis to characterize an input function. In addition, any reference tissue models may have difficulty with very noisy data particularly for pixel time activity curves (TACs) in parametric imaging owing to a poor brain uptake of [^{11}C]PK-11195. In the present study, we evaluated the PBRs binding in a rat brain injury model using [^{11}C]PK-11195 and animal PET with regions of interest (ROIs)-based approach to estimate V. We used an integral from 0 min to 60 min (V_{60}) as an estimate of V and differences in right/left ST V_{60} ratios between lesioned and unlesioned control rats. The PET findings were then compared with qualitative immunohistochemical findings.

Materials and methods

Preparation of [^{11}C]PK-11195

[^{11}C]PK-11195 was prepared from enantiomerically pure desmethyl precursor following the method reported earlier [11]. [^{11}C]methyl iodide, which was obtained using the conventional $LiAlH_4$ method, was trapped in 0.3 ml of NaOH/DMSO suspension containing (R)-*N*-desmethyl PK-11195 PLUS (1 mg, ABX, Dresden, Germany). The mixture was then heated at 100°C for 3 min followed by high-performance liquid chromatography (HPLC) purification. The fraction corresponding to [^{11}C]PK-11195 was collected and evaporated to dryness in vacuo. The residue was dissolved in 0.25% solution of Tween 80 in physiological saline. The radiochemical yield of the synthesis was 20.3% ± 5.9% (13.1%–30.8%) with decay correction. Analytical HPLC revealed that radiochemical purity of the product exceeded 98% and the specific radioactivity was 68.2 ± 18.1 GBq/μmol (39.5–88 GBq/μmol) at the end of the synthesis.

Operating procedure

All the procedures were conducted in accordance with the Guidelines for the National Institutes of Health and Animal Experimentation of the Fujita Health University, School of Medicine.

A novel ethanol injury model established by Takeuchi et al. [12] inducing microglial increment was made as follows.

Wild-type male Fisher rats (8–9 weeks, Charles River, Japan) were used in this study. Rats were anesthetized by intraperitoneal injection (50 mg/kg) of pentobarbital and placed on a stereotaxic frame (Narishige, Japan). The scalp was cleaned with an iodine solution and incised on the midline, and the hole was made in the skull at the appropriate stereotaxic location using a micro-drill. Unilateral intrastriatal administration (right side) of 8 μl of ethanol was performed using a 10-μl Hamilton syringe [12]. Ethanol was infused into the right ST at a rate of approximately 1 μl/min. The stereotaxic coordinates of the target site was anterior = 0.4 mm, lateral = 3 mm, and ventral = 4.5 mm from the Bregma, according to the atlas of Paxinos and Watson [13]. After the injection, the needle was placed for additional 10 min, and then slowly withdrawn.

MRI study

Two days after the surgery (day 3), MRI was performed using a clinical MR equipment, SIGNA INFINITY EXCITE system (1.5 T, GE Healthcare, Milwaukee, WI, USA), and wrist coil (Q-WRIST, GE Healthcare) to detect the extent of injury on the rat right striatum (ST) without killing prior to the PET studies. We have developed feasible techniques that can obtain high-resolution rat brain images to identify the ST stereotactically in a consistent and repetitive manner with neither high magnetic field MR imaging system nor stereotaxtic device dedicated for rodent. The positioning principle of our technique which consists of three-plane localization method based on the MR images utilizes the localization principle of the widely used rat brain atlas by Paxinos and Watson [13].

Briefly, rat skull surface was exposed and Bregma was identified. Copper sulfate solution in 10 mm hematocrit glass tube sealed bilateral ends for MR marker and was secured with tissue adhesive right above the Bregma under chloral hydrate (300 mg/kg) i.p. injection anesthesia. Rat head, body, arms, and legs were then fixed using surgical tape with prone position on acryl plate. The rat head on the acryl plate was inserted into the suitable size wrist coil, which was applicable for small radio frequency head coil on the MRI scanner bed.

First three planes (axial, coronal, and sagittal sections) were taken simultaneously (TR/TE = 55.3/1.8 FOV = 12 × 12 cm) for 44 s; then accurate sagittal planes were acquired on the basis of these three planes correcting the tilt on the horizontal plane (TR/TE = 300/9.2 FOV = 12 × 12 cm) for 69 s. Bilateral external auditory meatus, which determine the interaural line, incisor bar, and Bregma marker were identified on these sagittal planes. Seven T2-weighted coronal images (TR/TE = 2000/102 FOV = 10 × 5 cm, 17 echo train length) for 3 min and 48 s were then taken rectangular to the plane between interaural line and incisor bar. A third slice image from the front was set on the Bregma marker which corresponds to the ST plane (Fig. 1). The slice thickness was 3 mm. Image matrix was 320 × 256.

We performed five ethanol-injured rats in one experiment day and scanned using MRI. We performed following PET scanning only for rats which showed high-intensity area around the ethanol-injected right ST on the T2-weighted images (Fig. 1).

PET study

We used the SHR-2000 animal PET device (Hamamatsu Photonics, Hamamatsu, Japan), which provides a 14-slice image set with a maximal image spatial resolution of 3.5 mm full width at half maximum [14].

The next day (day 4), we performed PET scanning for 17 ethanol-injured rats (159–203 g, 180.2 ± 16.2 g) and 7 non-treated rats (125–240 g, 158.2 ± 46.9 g) for control.

A 24-G indwelling needle (Terumo, Tokyo, Japan) was inserted into the tail vein under light ether anesthesia, and then chloral hydrate (300 mg/kg) was intraperitoneally injected into rats. Under anesthesia the rat head was fixed using an originally designed acrylic head holder by modifying a stereotaxic holder used in physiological experiments (Hamamatsu Photonics) [15] based on the rat brain atlas by Paxinos and Watson [13]. The positioning principle was a three-point fixation, consisted of two earplugs and incisor bar [16]. Correction of photon

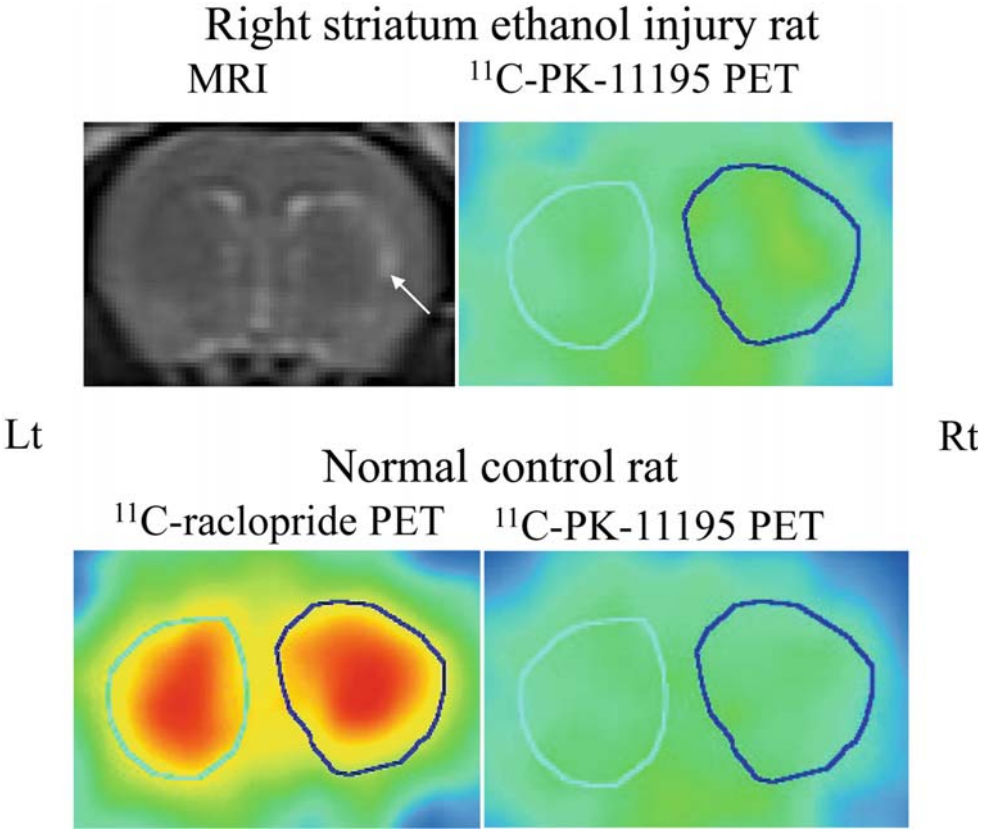

Fig. 1 Representative coronal magnetic resonance imaging (MRI) T2-weighted images (*arrow* in *left top row* showing ethanol injury lesion), summed images (0–60 min) of ^{11}C-PK-11195 positron emission tomography (PET) in ethanol-injured rat (*top row right*) and normal control rat (*bottom row right*) and ^{11}C-raclopride PET (*bottom row left*) with regions of interest on bilateral striatum

attenuation was carried out with transmission data obtained by rotating the ^{68}Ge/^{68}Ga rod source for 15 min.

Dynamic PET scans (24 frames; frames 8 × 30 s, 6 × 60 s, 10 × 300 s) were acquired for 60 min under continuous infusion of chloral hydrate (100 mg/kg per hour) immediately following a bolus injection of 13–39 MBq of [^{11}C]PK11195 through the tail vein. The body temperature in the anesthetized animals was monitored with a rectal temperature probe and maintained at 31.2–36.5°C with a heating pad. The scanned images of [^{11}C]PK11195 were reconstructed using a Butterworth filter with a cut-off frequency of 144 cycle/cm [17]. The slice thickness was 3 mm. A third slice image from the front was set on the Bregma which corresponds to the ST plane.

PET data analysis

Regions of interest on bilateral ST were placed on the reconstructed images guided by the rat brain atlas by Paxinos and Watson [13], and the reports of Suzuki and Sakiyama [15, 16] (Fig. 1). [^{11}C]raclopride imaging for dopamine D2 receptor was performed to validate the accuracy of ST slice based on our stereotaxic three-point fixation for pilot study and used to delineate ROI on bilateral ST for reference (Fig. 1). ROI values on bilateral ST were divided by the injection dose (kBq) to obtain an image ROIs-derived [^{11}C]PK11195 percentage of the injected dose per gram of tissue (%ID/g), and were multiplied by the whole body weight (in kg) to determine body-weight normalized radioactivity concentration (%ID-kg/g).

For the pilot study, we tried kinetic modeling for four rats using arterial input functions and metabolite analysis to measure the distribution volume and binding potential. However, any kinetic analyses had difficulty with very noisy data particularly for pixel TACs in parametric imaging owing to a poor brain uptake of [^{11}C]PK-11195 relatively arterial blood data (data not shown). In the present study, we evaluated the PBRs binding with ROIs-based approach to estimate an index of [^{11}C]PK-11195 total distribution volume (V).

The total distribution volume can be defined as follows [18]:

$$V = \frac{\int_0^\infty \mathrm{ROI}\, dt}{\int_0^\infty \mathrm{Plasma}\, dt}$$

; a ratio of ROI area under the curve (AUC)-to-plasma AUC to time infinity. In the present study, we used an integral from 0 min to 60 min (V_{60}) as an estimate of V. V_{60} underestimates V (i.e., $V_{60} < V$), because plasma time activity clears more rapidly than does the ROI time activity. We used V_{60} of the ST of injected side normalized by V_{60} of the uninjected side as an outcome measure, which should be increased if [^{11}C]PK-11195 binding is increased because of inflammation on the injected side, assuming that the underestimation of V by the use of V_{60} is similar on both sides. Thus, we calculated V_{60}(right ST)/V_{60}(left ST) = (right ST AUC/plasma AUC)/(left ST AUC/plasma AUC) = right ST AUC/left ST AUC. Therefore, the calculation of this ratio eliminated the need for blood data. We then compared this ratio between lesioned and unlesioned control rats. The level of statistical significance was designated as $P < 0.05$.

Tissue preparation and histochemical staining

On the PET experiment day (day 4) after the scanning, Fisher rats were deeply anesthetized with pentobarbital (25 mg/kg, i.p.) and exsanguinated by transcardial perfusion with isotonic saline solution, and brains were removed after decapitation. The brain was isolated, frozen in liquid nitrogen, and embedded in OCT compound (Tissue-Tek; Sakura Finetek, Tokyo, Japan). Frozen sections (8 μm) were serially cut into four slices using a microtome (Laica, Solms, Germany), then transferred to gelatin-coated slides and air dried. The sections were fixed with 4% paraformaldehyde in PBS at 4°C for 15 min to determine the location of exogenous microglia relative to the ST area. Sections were labeled with FITC-conjugated Griffonia simplifolia isolectin-B4 (IB4-lectin) (GSA-IB4; Sigma, St. Louis, MO, USA), monoclonal antibodies against ED-1 (Rat leukocyte antigen; BMA, Augst, Switzerland) or ED-2 (rat macrophage antigen; BMA). In brief, sections were incubated for 30 min at room temperature in PBS containing 1% bovine serum albumin, 10% normal goat serum, and 0.01% sodium azide, and then labeled with a monoclonal antibody against ED-1 at a dilution of 1:100 or the ED-2 at a dilution of 1:100. The reaction was visualized with FITC-conjugated goat F(ab9)2 anti-mouse IgG (Rockland) at a dilution of 1:200, and then photographed under a fluorescent microscope (BX-50, Olympus, Tokyo, Japan). Each serial section was stained using hematoxylin–eosin (HE).

Visual interpretations of representative slices of the ST were performed. Quantification of immunohistochemical evaluations was not carried out because quantification of representative thin histochemical slice sections (8 μm) may not be equivalent to the thicker slice thickness (3 mm) PET data.

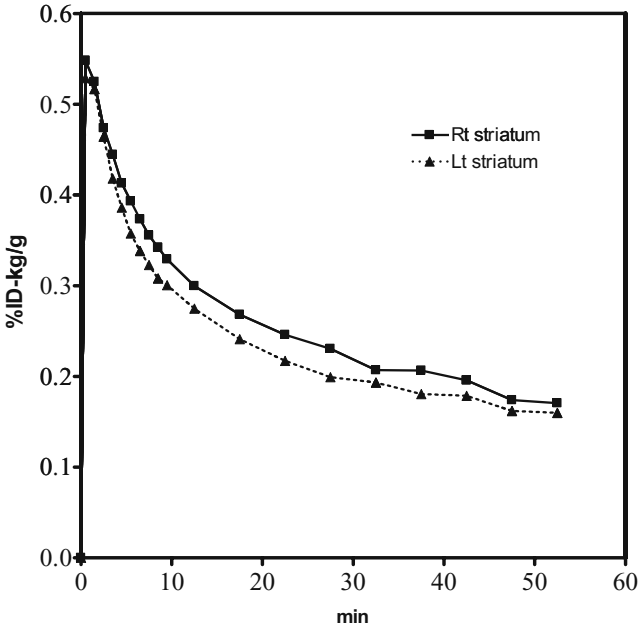

Fig. 2 Averaged time–activity curves of [^{11}C]PK-11195 in lesioned right and unlesioned left striatum in injury rats. For clarity, these figures do not show error bars and are meant to convey only trends

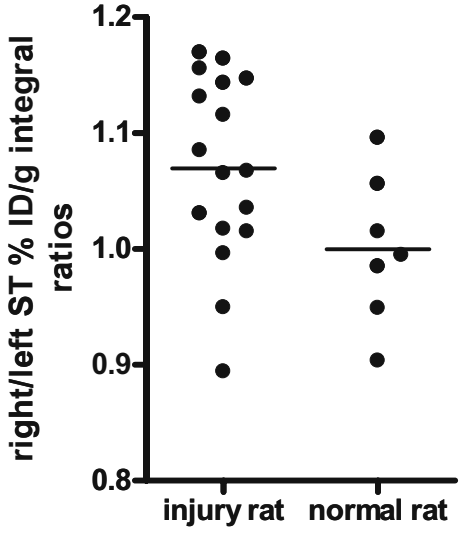

Fig. 3 Comparison of 0–60 min right/left ST %ID/g integral ratios (right/left ST V_{60} ratios) between injury and unlesioned control rats in [^{11}C]PK-11195 brain PET. The ratios in lesioned rats (1.07 ± 0.08) are significantly higher than in unlesioned control rats (1.00 ± 0.06, $P < 0.05$)

Results

PET data analysis

Averaged TACs showed rapid entry and clearance of [^{11}C]PK-11195 in lesioned and unlesioned ST in injury rats (Fig. 2). The highest peaks were 0.56 ± 0.22 %ID-kg/g (3.1 ± 1.14 %ID/g) in lesioned right ST and 0.54 ± 0.23 %ID-kg/g (3.0 ± 1.15 %ID/g) in unlesioned left ST at 0.5 min. There were no significant differences in averaged peak %ID-kg/g values between lesioned and unlesioned ST. In the time course of [^{11}C]PK-11195 activity, [^{11}C]PK-11195 clearance in lesioned right ST was slower than that in unlesioned left ST (Fig. 2).

The 0–60 min right/left ST %ID/g integral ratios (right/left ST V_{60} ratios) in lesioned rats (1.07 ± 0.08) were significantly higher than those in unlesioned control rats (1.00 ± 0.06, $P < 0.05$, Fig. 3).

Histochemical staining of lesioned rats

In HE, a faintly stained, cavernous necrotic area showing coagulation of the tissue and loss of neuronal and glial cells was present around the injected wound in the right ST. On immunohistochemical staining, IB4-lectin and ED-1 positive cells showing activated microglia were exclusively detected in boundary area of the ethanol-injected region in the right ST but neither in the non-lesioned left ST of the lesioned rats nor in the bilateral ST of the non-lesioned control rats (Fig. 4). To characterize the immunohistochemically stained cells, we double-stained with ED-1 and ED-2. ED-2 that stain macrophage did not stain cell even though activated microglia were detected with ED-1 in lesioned right ST.

Discussion

In this study, [^{11}C]PK-11195, a PET ligand for PBR showed increased binding as expressed in affected/non-affected ST integral ratios (0–60 min, right/left ST V_{60} ratios) between lesioned and unlesioned control rats. These findings are consistent with activated microglia in a rat brain ethanol injury model. The microglia activation was also confirmed by the immunohistochemical staining in the present study.

Price et al. [19] reported that in the ST of sham-lesioned rats [^{3}H]PK-11195 entered brain rapidly, with maximal brain radioactivity occurring within of 2 min of injection and then cleared rapidly. These investigators did not use PET imaging. Rather, they made tracer uptake measurements of dissected brain in a scintillation counter at each time point. They found that the clearance of [^{3}H]PK-11195 in lesioned ST was slower than that in unlesioned ST. In our PET imaging of injury rats, the findings of rapid entry (the highest peaks at 0.5 min) and clearance of [^{11}C]PK-11195 in lesioned and

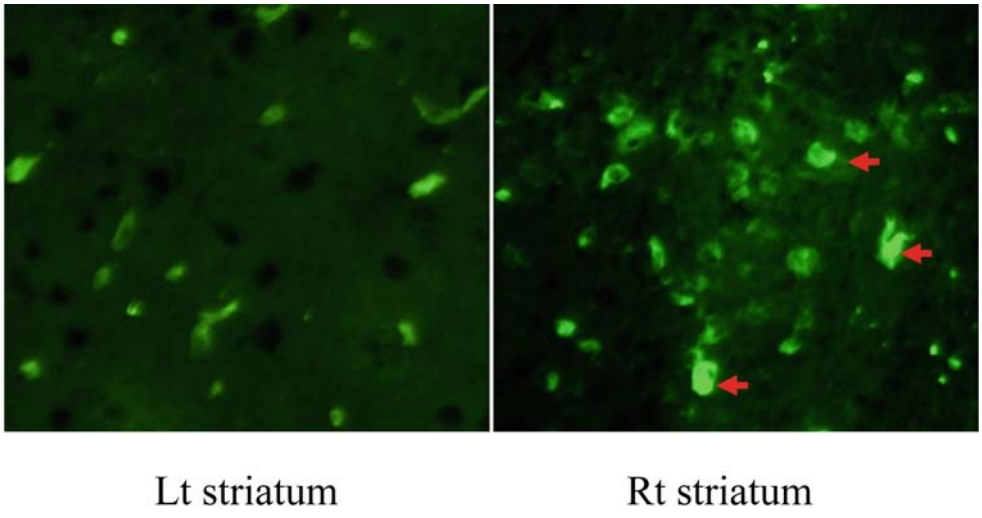

Fig. 4 Immunohistochemical staining (IB4-lection stain) on the lesioned right and unlesioned left striatum in the same lesioned rat model. Activated microglia are shown in the lesioned right striatum (*arrows*), but not shown in the unlesioned left striatum

unlesioned ST and slower clearance in lesioned ST than in unlesioned ST are consistent with their ex vivo findings. Cicchetti et al. [5] calculated binding ratios of [^{11}C]PK-11195 between ST and cerebellum with percentage activity of injected dose per pixels in a Parkinson disease rat model induced by unilateral intrastriatal administration of 6-hydroxydopamine using PET. They showed increased [^{11}C]PK-11195 binding by 67% in the lesioned ST and microglial response by immunohistochemistry [5]. In our ethanol injury model, the 0–60 min right/left ST %ID/g integral ratios (right/left ST V_{60} ratios) in lesioned rats were significantly higher than those in unlesioned control rats. However, these differences were only around 7%. In our ethanol injury model, the signal of [^{11}C]PK-11195 in the brain may not be high enough because of low uptake into the brain [8, 9]. Relatively low resolution of our PET scanner might also influence the result of low signal differences. We have obtained rat ST slices on MRI using the three-plane localization method and [^{11}C]PK-11195 PET using stereotaxtic device confirmed by [^{11}C]raclopride uptakes stereotactically for both third slices from the top. Although there are no changes in the ST volume secondary to lesioning, so partial volume should be of the same degree for both sides, accurate MRI and PET fusion techniques would be warranted in the future for much more limited ROI setting on the ethanol injury lesion on the ST using a better resolution PET scanner with less partial volume effect on thinner slice thickness.

Because there is scattering in right/left ST V_{60} ratios in both injury and normal rats, manual ROI setting on bilateral ST might influence the values. Recently, our experiment has shown that increased [^{11}C]PK-11195 binding might be closely related to toxic conversion of activated micloglia not just only the number of activated microglia (data not shown). Inflammatory cytokines for markers of toxic conversion might be significant to subdivide the widely varied right/left ST V_{60} ratios in injury rats.

An initial PET study using [^{11}C]PK-11195 evaluated with average counts per voxel normalized to cerebellum also showed no detectable alteration in patients with mild to moderate AD probably because of low specific to non-specific binding ratios in mild to moderate AD [10]. However, the Hammersmith hospital group has developed cluster analysis to calculate binding potential for the extraction of voxels with normal ligand kinetics to serve as the reference input function which voxels in the raw dynamic data are segmented into 10 clusters distinguished by the shape of their TACs [1, 20]. They showed significantly increased regional [^{11}C]PK-11195 binding in patients with mild to moderate AD and minimal cognitive impairment [6]. Their cluster analysis might be useful to detect faint signal of [^{11}C]PK-11195 specific binding. Reference tissue models for the analysis of [^{11}C]PK-11195 have also been reported recently [21, 22]. However, they pointed a limitation of this study for using the cerebellum as a reference tissue because increased specific binding in these structures cannot be excluded [21, 22]. In this rat experiment with small brain and limited number of voxels involved, rather than cluster analysis or reference tissue models, we sought to estimate a more direct measure of PBRs receptor binding by an ROIs-based approach to estimate distribution volume. Strictly speaking, infinity scanning time (practically impossible) should be applied to estimate distribution volume with our ROIs-based approach. In the present study, V_{60} was used as an index of V. V_{60} unlike V is affected to some extent by blood flow. In addition, V_{60} which is calculated as ROI AUC includes the activity

in the brain vascular compartment. Therefore, the increased V_{60} ratio could be partly explained by the possibility that blood flow is increased on the lesioned side. However, there were no significant differences in averaged peak %ID-kg/g values between lesioned and unlesioned ST. The lesioned side may have increased flow, and washout is then expected to be faster. However, the lesioned side shows a similar washout rate to the unlesioned side (Fig. 2). Therefore, the difference in TACs in Fig. 2 is consistent with higher binding in the lesioned side.

Takeuchi et al. [12] have established a novel injury model in the CNS by a stereotaxic injection of ethanol into rat ST to induce necrosis. They first demonstrate that microglial inducible nitric oxide synthase (iNOS) mRNA was induced in vivo after the injury and microglial iNOS is considered to play a pivotal role in eliminating damaged neurons by apoptosis, thereby protecting neuronal circuits from necrotic damage [12]. Barger and Harmon [23] showed that microglia in vitro activated by Alzheimer's amyloid precursor protein release NO via iNOS induction. Thus, microglia in vivo may reveal neurotoxic effects via producing NO under certain conditions [12]. Some advantages of our injury model are that the stereotaxic operation seems to produce less damage to other places in the brain than other models such as needle-penetrating wounds, and suction on the brain surface [24, 25]; and necrotic damage seems to be free from hemorrhage and infection owing to the coagulating and sterilizing effects of ethanol [12]. We performed PET scanning for only those rats that showed a high intensity area around the ethanol injected right ST on the T2-weighted images for the ideal injury model. However, in double staining with ED-1 and ED-2, positive cells showing activated microglia were detected in the injured right ST with ED-1, but ED-2 that stains macrophage did not stain cell. Increased PBRs binding in our model would represent the activated microglia, and not owing to macrophages that have crossed through blood–brain barrier leakage. We have not performed the quantification for the immunohistochemical evaluation as mentioned in "Materials and methods". We will compare between the number of activated microglia equivalent to PET slices and PBR binding on PET in the future work.

Recently, novel PET PBRs ligands such as [^{11}C]DAA 1106 [26, 27] and [^{11}C]PBR28 [28, 29] which have higher specific binding compared with [^{11}C]PK-11195 have been developed. Higher specific binding ligands to PBR would be expected to have higher sensitivity of the detection of over expression of PBRs binding sites in the activated microglial cells following injury or degeneration in the brain using in vivo PET imaging.

Conclusions

In this study, [^{11}C]PK-11195, a PET PBR ligand showed increased binding as expressed in affected/non-affected ST integral ratios (0–60 min) between lesioned and control rats consistent with activated microglia in a rat brain ethanol injury model.

These results suggest that [^{11}C]PK-11195 PET imaging and our ROIs-based approach to estimate distribution volume might be a useful tool to evaluate in vivo microglial activation in a rat brain injury model.

Acknowledgments We thank Mr. Junichiro Abe, Department of Brain Science and Molecular Imaging, National Institute for Longevity Sciences, Obu, Japan, for running the cyclotron. We appreciate Mr. Masao Ohashi, RT and other radiological technologists for running the MRI scanner and valuable suggestions.This research was supported in part by Japan Society for the Promotion of Science (JSPS) KAKENHI (18591369), the 21st Century COE (Center of Excellence) Medical Program (Development Center for Targeted and Minimally Invasive Diagnosis and Treatment) from JSPS and a grant from Fujita Health University and Suzuken Memorial Foundation.

References

1. Banati RB. Visualizing microglial activation in vivo. Glia 2002;40:206–17.
2. Stoll G, Jander S. The role of microglia and macrophages in the pathophysiology of the CNS. Prog Neurobiol 1999;58:233–47.
3. Banati RB, Egensperger R, Maassen A, Hager G, Kreutzberg GW, Graeber MB. Mitochondria in activated microglia in vitro. J Neurocytol 2004;33:535–41.
4. Ladeby R, Wirenfeldt M, Garcia-Ovejero D, Fenger C, Dissing-Olesen L, Dalmau I, et al. Microglial cell population dynamics in the injured adult central nervous system. Brain Res Brain Res Rev 2005;48:196–206.
5. Cicchetti F, Brownell AL, Williams K, Chen YI, Livni E, Isacson O. Neuroinflammation of the nigrostriatal pathway during progressive 6-OHDA dopamine degeneration in rats monitored by immunohistochemistry and PET imaging. Eur J Nerurosci 2002;15:991–8.
6. Cagnin A, Brooks DJ, Kennedy AM, Gunn RN, Myers R, Turkheimer FE, et al. In-vivo measurement of activated microglia in dementia. Lancet 2001;358:461–7.
7. Hammoud DA, Endres CJ, Chander AR, Guilarte TR, Wong DF, Sacktor NC, et al. Imaging glial cell activation with [^{11}C]-R-PK 11195 in patients with AIDS. J Neurovirol 2005;11:346–55.
8. Debruyne JC, Van Laere KJ, Versijpt J, De Vos F, Eng JK, Striickmans K, et al. Semiquantification of the peripheral-type benzodiazepine ligand [^{11}C]PK11195 in normal human brain and application in multiple sclerosis patients. Acta Neurol Belg 2002;102:127–35.
9. Zhang MR, Maeda J, Ogawa M, Noguchi J, Ito T, Yoshida Y, et al. Development of a new radioligand, *N*-(5-fluoro-2-phenoxyphenyl)-*N*-(2-[^{18}F]fluoroethyl-5-methoxybenzyl) acetamide, for PET imaging of peripheral benzodiazepine receptor in primate brain. J Med Chem 2004;47:2228–35.

10. Groom GN, Junck L, Foster NL, Frey KA, Kuhl DE. PET of peripheral benzodiazepine binding sites in the microgliosis of Alzheimer's disease. J Nucl Med 1995;36:2207–10.
11. Shah F, Hume SP, Pike VW, Ashworth S, McDermott J. Synthesis of the enantiomers of [*N*-methyl-^{11}C]PK 11195 and comparison of their behaviors as radioligands for PK binding sites in rats. Nucl Med Biol 1994;21:573–81.
12. Takeuchi A, Isobe KI, Miyaishi O, Sawada M, Fan ZH, Nakashima I, et al. Microglial NO induces delayed neuronal death following acute injury in the striatum. Eur J Neurosci 1998;10:1613–20.
13. Paxinos G, Watson C. The rat brain in stereotaxic coordinates. 4th ed. San Diego: Academic; 1998.
14. Watanabe M, Uchida H, Okada K, Shimizu K, Satoh N, Yoshikawa E, et al. A high resolution PET for animal studies. IEEE Trans Med Imaging 1992;11:577–80.
15. Suzuki M, Hatano K, Sakiyama Y, Kawasumi Y, Kato T, Ito K. Age-related changes of dopamine D_1-like and D_2-like receptor binding in the F344/N rat striatum revealed by positron emission tomography and in vitro receptor autoradiography. Synapse 2001;41:285–93.
16. Sakiyama Y, Hatano K, Tajima T, Kato T, Kawasumi Y, Suzuki M, et al. An atlas-based image registration method for dopamine receptor imaging with PET in rats. Ann Nucl Med 2007;21:455–62.
17. Momosaki S, Hatano K, Kawasumi Y, Kato T, Hosoi R, Kobayashi K, et al. Rat-PET study without anesthesia: anesthetics modify the dopamine D_1 receptor binding in rat brain. Synapse 2004;54:207–13.
18. Lassen NA. Neuroreceptor quantitation in vivo by the steady-state principle using constant infusion or bolus injection of radioactive tracers. J Cereb Blood Flow Metab 1992;12:709–16.
19. Price GW, Ahier RG, Hume SP, Myers R, Manji L, Cremer JE, et al. In vivo binding to peripheral benzodiazepine binding sites in lesioned rat brain: comparison between [^{3}H]PK11195 and [^{18}F]PK14105 as markers for neuronal damage. J Neurochem 1990;55:175–85.
20. Gunn RN, Lammertsma AA, Hume SP, Cunningham VJ. Parametric imaging of ligand–receptor interactions using a reference tissue model and cluster analysis. In: Carson R, Daule M, Witherspoon P, Herscovitch P, editors. Quantitative functional brain imaging with positron emission tomography. San Diego: Academic; 1998; p. 401–6.
21. Kropholler MA, Boellaard R, Schuitemaker A, Folkersma H, van Berckel BNM, Lammertsma A. Evaluation of reference tissue models for the analysis of [^{11}C](R)-PK11195 studies. J Cereb Blood Flow Metab 2006;26:1431–41.
22. Schuitemaker A, van Berckel BNM, Kropholler MA, Veltman DJ, Scheltens P, Jonker C, et al. SPM analysis of parametric (R)-[^{11}C]-PK11195 binding images: plasma input versus reference tissue parametric methods. Neuroimage 2007;35:1473–79.
23. Barger SW, Harmon AD. Microglial activation by Alzheimer amyloid precursor protein and modulation by apolipoprotein E. Nature 1997;388:878–81.
24. Cavanagh JB. The proliferation of astrocytes around a needle wound in the rat brain. J Anat 1970;106:471–87.
25. Finklestein S, Campbell A, Stoll AL, Baldessarini RJ, Stinus L, Paskevitch PA, et al. Changes in cortical and subcortical levels of monoamines and their metabolites following unilateral ventrolateral cortical lesions in the rat. Brain Res 1983;271:279–88.
26. Zhang MR, Kida T, Noguchi J, Furutsuka K, Maeda J, Suhara T, et al. [^{11}C]DAA1106: radiosynthesis and in vivo binding to peripheral benzodiazepine receptors in mouse brain. Nucl Med Biol 2003;30:513–9.
27. Maeda J, Suhara T, Zhang MR, Okauchi T, Yasuno F, Ikoma Y, et al. Novel peripheral benzodiazepine receptor ligand [^{11}C]DAA1106 for PET: an imaging tool for glial cells in the brain. Synapse 2004;52:283–91.
28. Imaizumi M, Kim HJ, Zoghbi SS, Briard E, Hong J, Musachio JL, et al. PET imaging with [^{11}C]PBR28 can localize and quantify upregulated peripheral benzodiazepine receptors associated with cerebral ischemia in rat. Neurosci Lett 2007;411:200–5.
29. Imaizumi M, Briard E, Zoghbi SS, Gourley JP, Hong J, Musachio JL, et al. Kinetic evaluation in nonhuman primates of two new PET ligands for peripheral benzodiazepine receptors in brain. Synapse 2007;61:595–605.